AI Integrated Environmental Monitoring for Heat Stress Management in Healthcare and Public Spaces

Manvendra Deswal[1*], Rajkumar Balasubramaniam[1], Abhinav Raj[1], Sadaksh Arora[1], Sarthak Belekar[1]

[1] Innovant & Inspired Living Solutions (I2L), Pune, Maharashtra, India.
*manvendra@i2l.net , rajkumar@i2l.net , abhinavraj.ssg5586@gmail.com, sadaksh@ids-pl.com , sarthak@i2l.net

Abstract. Extreme heat events are increasing in frequency, intensity, and duration under climate change with a mean global temperature rise of 1.2 °C having arisen from increasing greenhouse gas emissions. This effect threatens public health in densely populated regions such as India. In this paper, an AI based environmental monitoring system for the prediction and control of heat stress in healthcare and educational settings is discussed. This study utilized machine learning (Random Forest, Gradient Boosting, CatBoost and SVR) and deep learning (LSTM) models to predict the Heat Index (HI), an apparent ("feels-like") temperature derived from air temperature and relative humidity, using a five-year high-resolution meteorological dataset from a hospital campus in Gurugram, India, and to analyze the temporal dynamics of heat stress.[16] A multiple correlation analysis showed that the radiation and humidity parameters (especially longwave irradiance, wet bulb temperature, and UVB irradiance) had a significant effect on perceived thermal stress; >43% of observed hours were in categories of "danger" or "extreme caution". The Random Forest model achieved the highest predictive performance ($R^2 = 0.9993$, RMSE = 0.3231), indicating strong nonlinear mapping and good generalization on the test set. The LSTM captured sequential dependencies in the time series ($R^2 = 0.973$, RMSE = 1.797) but showed higher error than the tree-based models under the present dataset and training configuration. These predictive outputs are embedded within a proactive heat stress management workflow that includes automated warnings, HVAC operational adjustments, and nature-based cooling measures such as shaded pathways and green roofs. Consistent with prior field evidence, such interventions can reduce heat stress exposure (often reported using WBGT) and improve operational resilience in high risk periods.

Keywords: AI integration, Environmental monitoring, Heat stress, Healthcare management, Public spaces

1 Introduction

Global climate change has increased the frequency and severity of heatwaves, leading to significant health and economic impacts [11]. South Asia has the highest increase, as heat related mortality is estimated to be fourfold by 2050 [5]. India is one of the worst

A. Vaidya et al. (eds.), *Proceedings of the Conference on Bioengineering for Global Health (SYMRESEARCH 2.0 2025)*, Advances in Biological Sciences Research 55,
https://doi.org/10.2991/978-94-6239-756-9_27

affected countries, having witnessed a 3 fold increase in the number of annual heatwave days over the past 30 years with a temperature as high as 47° C and above [1].For instance, Maharashtra has already warmed by 0.6°C since 1901 and projected to witness an increase in maximum temperatures spanning from 1.5 2°C by 2050 [4]. The elderly, children and those workers who will be working outside make up most of the susceptible population that is affected by increasing productivity losses and an estimated 4.5% reduction in the nation's GDP [6]. Current Heat Action Plans are predominantly reactive, have minimal local forecasting and poor linkages between health and environmental data. Extreme heat poses an immediate operational and public health risk for healthcare campuses, where vulnerable patients, visitors, and staff can experience hazardous thermal exposure during routine movement and service delivery. However, current Heat Action Plans and facility responses are often reactive and are rarely supported by localized, high resolution monitoring and short-term forecasting that can trigger timely, campus level actions. To address this gap, this study proposes an AI integrated environmental monitoring framework that combines sensor based microclimate observations (air temperature, relative humidity, wind speed, solar irradiance, and pressure) with predictive models to forecast heat stress conditions and characterize temporal risk patterns. Using five years of hourly observations from a hospital campus in Gurugram, India, we benchmark machine learning (Random Forest, Gradient Boosting, CatBoost, SVR) and deep learning (LSTM) models and link the predictions to actionable response pathways, including automated alerts, HVAC operational adjustments, and nature based cooling measures. In this paper, Heat Index (HI) is used as the primary prediction target for public heat risk communication, while Wet Bulb Globe Temperature (WBGT) is referenced as a complementary indicator in the literature and mitigation discussion because it incorporates radiant heat and wind effects and is widely used in occupational heat stress guidance.

2 Literature Review

2.1 Heat stress indices and standards (HI vs WBGT)

Heat stress is commonly characterized using composite indices that translate meteorological exposure into physiologically meaningful "felt" heat. The **Heat Index (HI)** combines **air temperature and relative humidity** to approximate perceived heat under typical outdoor conditions; standard formulations assume shaded conditions, and perceived heat can increase under direct sun exposure.[1][2] In India, the India Meteorological Department (IMD) similarly describes heat discomfort as a function of temperature and humidity and explicitly defines HI in this context.[2]

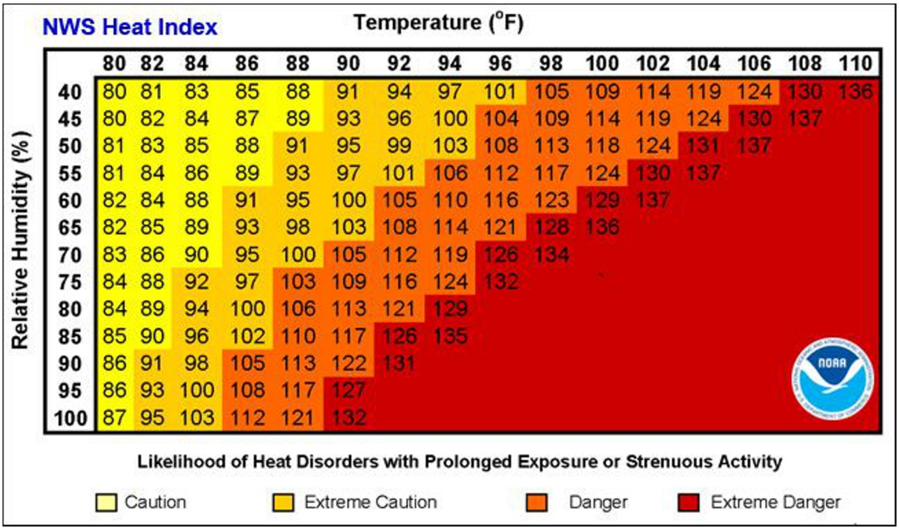

Fig. 1. Heat index chart (Source: National Weather Service)

For occupational and high-exertion settings, the **Wet Bulb Globe Temperature (WBGT)** is widely used because it better reflects combined heat loads (including radiant heat) relevant to work–rest cycles and safety thresholds. International guidance formalizes WBGT-based screening for heat stress during an occupational workday (up to 8 hours) through **ISO 7243**, and complementary occupational-health guidance is provided in the **NIOSH criteria standard** for heat exposure.[3][4]. This study uses **HI as the primary predictive target** because HI can be computed reliably from routinely available meteorological variables (temperature and relative humidity) and directly supports public-health messaging and facility operations. **WBGT is retained in the review** to anchor the discussion in established occupational standards and to contextualize mitigation actions for outdoor workers and high-risk operational roles. [3][4].

2.2 India/South Asia heat risk and Heat Action Plan (HAP) gaps

Indian cities face increasing heat-health risks, motivating the adoption of Heat Action Plans (HAPs) that integrate early warnings, public advisories, and health-system readiness. The Ahmedabad HAP is widely cited as a foundational South Asian example; its development emphasized local thresholds, inter-agency coordination, and actionable communication pathways.[5] Evidence from a pilot evaluation of Ahmedabad's HAP indicates measurable changes in heat-related outcomes, supporting the broader case for institutionalizing heat governance through HAPs.[6] However, synthesis work also highlights persistent implementation and governance gaps across cities—such as uneven attention to WHO core elements, limited formal evaluation, and inconsistent institutional arrangements for inter-sectoral coordination and health surveillance. A

recent assessment of HAPs across eight Indian cities explicitly frames these gaps against WHO's heat–health action guidance and identifies opportunities to strengthen heat governance.[7][8] National guidance from NDMA also emphasizes multi-stakeholder coordination, granular data collection, surveillance, and iterative plan improvement; NDMA notes that guidelines for heat action planning were issued in 2016 and revised subsequently, alongside emphasis on long-term mitigation measures.[9]
Literature indicates that HAP effectiveness depends not only on hazard forecasts but also on locally relevant risk indicators, trigger thresholds, and operationally implementable actions (especially for critical facilities and vulnerable populations). [6, 7, 9]

2.3 AI/ML for heat risk prediction and early warning

Conventional early warning practice relies on numerical weather prediction and operational forecast bulletins, typically produced at district-to-subdivision scales and for lead times of several days, with recognition that humidity and other meteorological factors modulate impacts.[2] Recent research increasingly applies machine learning (ML) and deep learning (DL) approaches to improve forecast skill or extend lead time. For example, Ratnam et al. evaluate multiple ML models for predicting daily maximum temperature anomalies over India with ~10-day lead times during the pre-monsoon heat season.[10] At a sub-national scale, Suthar et al.[11] demonstrate ML-based prediction of maximum air temperature to support heat-wave occurrence definition in Indian states. Complementing meteorology-focused efforts, newer work explores decision-support systems that translate forecast outputs into user-relevant warnings, including "personalized" or intra-urban heat stress warning concepts.[12]. India also has emerging localized risk forecasting initiatives. ARTPARK, for instance, describes a deep-learning-based hyperlocal heat-health forecasting effort designed to provide sub-district risk guidance with up to ~10 days lead time and to integrate health and socio-demographic information for actionable advisories.[13]. Much of the published and operational work focuses on forecasting temperature or generic heat hazard at broad scales; comparatively fewer studies couple facility-scale environmental monitoring with predictive models for a public-health index (HI) and explicitly translate predictions into operational mitigation triggers suitable for healthcare and high-footfall public spaces.

2.4 Cooling and mitigation evidence (quantified reductions)

Mitigation literature indicates that microclimate modification and building/operational measures can substantially reduce thermal stress. Shading is consistently identified as a high-impact intervention for outdoor exposure: modeling and empirical evidence show that shade can reduce WBGT meaningfully, with reported reductions on the order of ~2–6°C depending on environment and exposure conditions.[14] At the building scale, cool-roof and roof-modification interventions have demonstrated measurable indoor benefits. In low-income housing in Ahmedabad, roof interventions produced peak-hour indoor temperature reductions ranging from approximately ~1.0°C (reflective coating) to ~4.5°C (modular roofing) relative to uncoated roofs, with other low-cost options showing intermediate reductions [15]. National guidance also reinforces the role of structural and operational measures (including cool roofs, surveillance, and facility readiness) as part of longer-term heat risk reduction planning [9]. A defensible heat-stress management framework should combine (i) a forecastable index such as HI for lead-time decision support, with (ii) mitigation actions whose benefits are supported by quantified evidence (e.g., shading and cool-roof measures), and (iii) facility-level protocols aligned with health-system preparedness and inter-agency coordination. Building on these strands, the present work positions its contribution at the intersection of (a) a public-health-relevant heat index (HI) suited to routinely available observations, (b) AI-enabled prediction models that can support actionable lead times, and (c) facility-ready mitigation actions supported by quantified evidence and aligned with HAP-oriented implementation needs. This addresses a practical gap in translating heat forecasts into operationally implementable heat-stress mitigation workflows for healthcare and high-occupancy public environments.

3 Proposed Framework

3.1 Framework overview and system architecture

This study proposes an AI-integrated heat-stress monitoring and response framework that converts campus microclimate observations into short-horizon HI forecasts and actionable heat-risk triggers for healthcare operations. The framework comprises (i) sensor-driven data acquisition, (ii) preprocessing and quality control, (iii) feature generation and storage, (iv) model inference, and (v) threshold-based alerting linked to operational response actions.

Sensors/data sources → Preprocessing & QC → Feature store → Model inference → Alert thresholds → Response actions

(a) Sensors/data sources: onsite meteorological station and/or BMS-linked weather feeds capturing air temperature, relative humidity, wind speed, pressure, and irradiance variables;

(b) Preprocessing & QC: timestamp alignment, missing-value handling, outlier screening, and unit harmonization;

(c) Feature store: engineered temporal and lag features (hour, month, season, and prior-hour meteorology), stored as an analysis-ready table;

(d) Model inference: ML/DL models generate HI forecasts for defined horizons;

(e) Alert thresholds: forecasts are mapped to risk bands (e.g., “caution”, “extreme caution”, “danger”) to activate triggers;

(f) Response actions: automated warnings and facility responses (cooling operations, shaded routing, hydration/rest guidance) are initiated based on forecast risk.

Problem formulation (forecast horizon and/or category output)
Let Xt denote the vector of microclimate variables observed at time t(e.g., temperature, humidity, wind speed, irradiance, and pressure) and let HI_tbe the corresponding Heat Index. The primary task is short-horizon forecasting, defined as:

$$\widehat{HI}_{t+\Delta} = f(X_t, X_{t-1}, \dots, X_{t-L+1}, \tau_t)$$

where Δis the forecast horizon (e.g., 1–6 hours), Lis the look-back window (e.g., 48 hours), and τ_tdenotes time features (hour-of-day, day-of-week, month, and season). In addition to continuous forecasting, the framework can optionally support a risk-category output by assigning (HI)^_(t+Δ) to operational bands (e.g., "extreme caution" and "danger") for decision triggering.
Training protocol (time-based split)
To preserve temporal integrity and avoid leakage, model development follows a time-ordered split:

Training set: January 2021 – December 2024
Validation set: January 2025 – March 2025
Test set: April 2025 – June 2025

Hyperparameters are selected using validation performance, and final results are reported on the held-out test period. Performance is evaluated using R^2, RMSE, and MAE, aligned with standard regression benchmarking.

Baseline models
Two baselines are included to contextualize model performance:
1 Persistence baseline (naïve forecast):

(HI)^_(t+Δ)=HI_t

This baseline reflects "no-change" behavior and is a standard reference for short-horizon forecasting.
2 Linear regression baseline: a linear mapping from predictors to HI, included as a transparent, low-complexity comparator (reported alongside other models).

3.2 Explainability and interpretability (SHAP)

To interpret model behavior and confirm physically consistent drivers of HI, the study uses SHapley Additive exPlanations (SHAP). SHAP values are computed for the best-performing tree-based model(s) (e.g., Random Forest, CatBoost) to quantify each feature's contribution to predictions at both global and local levels. The recommended primary visualization is a SHAP summary plot (beeswarm) showing feature importance and directionality across the test set, supplemented by dependence plots for key predictors (e.g., temperature, relative humidity, longwave irradiance).[17]

4 Methodology

This study adopts a mixed methods approach and Stats, combining technological deployment, predictive modeling, and community engagement and Methodology

4.1 Dataset

This study utilizes a five year high resolution (hourly) environmental dataset collected from a **hospital located in Gurgaon, Haryana, India (28.46°N, 77.07°E)**, representing an urban healthcare microclimate in northern India. The data span from **January 2021 to June 2025**, covering seasonal and interannual variations. The dataset includes key meteorological parameters such as air temperature (°C), relative humidity (%), surface pressure (kPa), wind speed (m/s), solar irradiance components (W/m²), precipitation (mm/hour), and derived thermal indices such as the Wet Bulb Temperature (WBT).

$$\boldsymbol{HI} = -42.379 + 2.04901523 * \boldsymbol{T} + 10.14333127 * \boldsymbol{RH} - 0.22475541 * \boldsymbol{T} * \boldsymbol{RH} - 0.00683783 * \boldsymbol{T}^2 - 0.05481717 * \boldsymbol{RH}^2 + 0.00122874 * \boldsymbol{T}^2 * \boldsymbol{RH} + 0.00085282 * \boldsymbol{T} * \boldsymbol{RH}^2 - 0.00000199 * \boldsymbol{T}^2 * \boldsymbol{RH}^2$$

T(°F) × RH (%)/100 (8) where T is temperature, °F, and RH is relative humidity.

HI was computed using the National Weather Service formulation based on the Rothfusz regression (SR 90-23), which is commonly applied for HI estimation from air temperature and relative humidity under typical operational conditions.[16], Missing and infinite values were filled forward to maintain temporal continuity by imputation. Furthermore, based on the date of death, temporal factors were obtained: hour of the day, day of the week, month, day in a year and season (winter–spring–summer–fall). All numerical data were normalized with either StandardScaler for traditional ML algorithms or MinMaxScaler in deep learning models to make feature distributions comparable.

4.2 Proposed Methodology

Data Cleaning

The original meteorological data set was treated with systematic preprocessing to achieve temporal consistency and analytical reliability. Hourly data of 2021–2025 were normalized by matching multi sensor inputs over common timestamps and fiducially adjusting temperature, humidity, wind speed, and irradiance parameters. Q Matrix Missing and infinite values were handled with forward fill imputation for maintaining chronological prompts. Due to longer term sensor drift and recording artifacts the outliers were detected based on z score thresholding and removed to maintain data integrity. Temperature was transformed into Fahrenheit to calculate the Heat Index, and derived time related features (hour, month and season) were used as well to account for daily and yearly variations. The last step was normalizing all the numerical columns using StandardScaler in case of machine learning models and MinMaxScaler in case of deep learning model, so features were uniformly scaled across the data set. These insights guaranteed that an observation was not overly averaged by season (since the previous months was integrated into the prediction) and reduced uniform noise while ensuring that a seasonal loop year does not introduce drift of dependencies, thus improving reliability of the model and reducing data driven bias in training/evaluation.

Feature Engineering and Derived Variables

For statistical reliability and dataset appropriateness for model building, diagnostic tests including P value significance check and Variance Inflation Factor (VIF) analysis were performed. The P value test was used to determine that all the major predictors had significant relationships with the dependent variable ($p < 0.05$) and VIF analysis was performed to assess collinearity among the features. The VIFs of variables with high values were transformed or not included to increase the stability and interpretability of the model. From these analyses, three separate datasets were generated to map more closely onto the structural and computational needs of various types of models:

A regression dataset comprising seven low collinearity features for Linear Regression and Support Vector Regression (SVR)
An ensemble dataset containing twelve optimized predictors for tree based and boosting algorithms such as Random Forest, Gradient Boosting, and CatBoost
A deep learning dataset with fourteen key features tailored for the LSTM neural network to capture temporal dependencies and nonlinear interactions.

Exploratory Data Analysis (EDA)

A full EDA (Exploratory Data Analysis) was carried out for the complete dataset to study the features distribution, interrelations and dynamics of thermal stress. Summary statistics suggested an average ambient temperature of approximately 25.21°C with a mean Heat Index of 88.45°F, describing warm weather conditions throughout the time period.Strong positive correlation was found between multiple tires of irradiance, particularly in the All Sky Surface Shortwave Downward Irradiance, UVA and UVB Irradiances and Top of Atmosphere Shortwave Downward Irradiance ($r > 0.90$), suggesting high multicollinearity among them because these responses relate to solar radiation intensity. On the other hand, Relative Humidity at 2 Meters was strongly negatively correlated with Temperature at 2 Meters ($r \approx -0.75$) and with all radiative variables, whose negative relation is physically reciprocal between humidity and temperature under clean sky conditions. There were moderate connections with the Surface Pressure and Solar Zenith Angle, detailing that it was an indirect influence from atmospheric stratification and solar position.

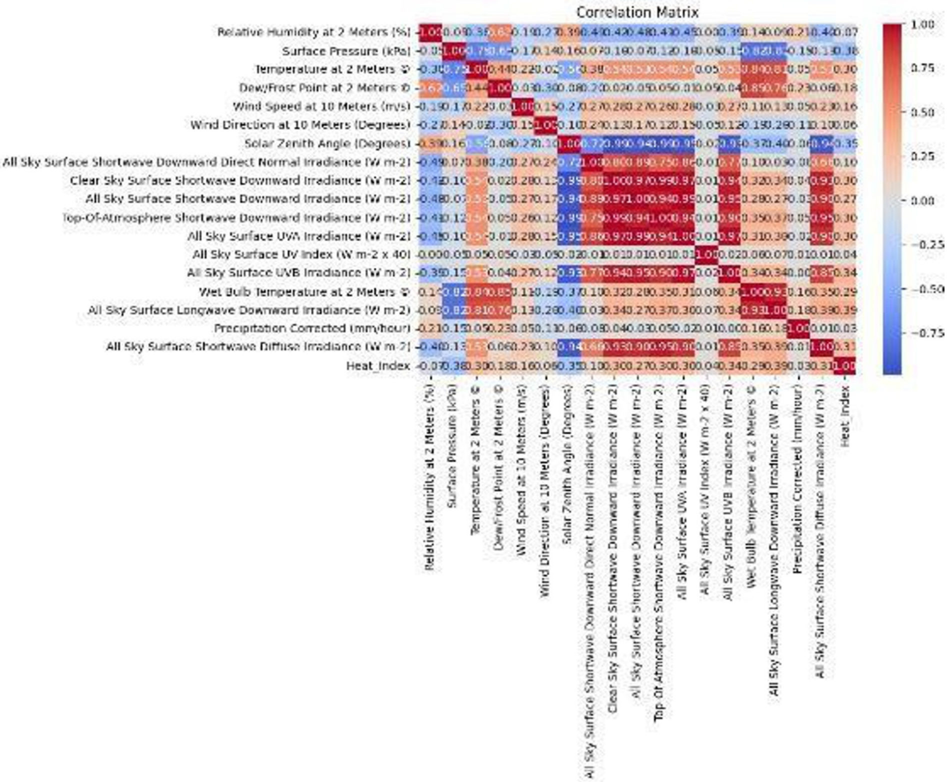

Fig. 2. Correlation Matrix

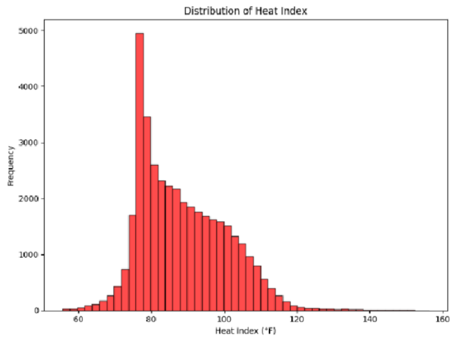

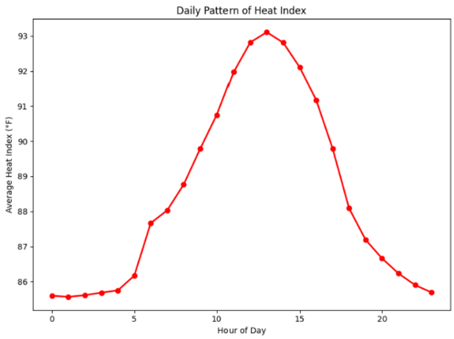

Fig. 3. Daily Pattern of Heat Index **Fig. 4.** Distribution of Heat Index

The Heat Index distribution is approximately right skewed, with a higher concentration of values around 75–95°F suggesting moderate climatic conditions and less frequency of extremely hot events above 110°F It can also be seen that the diurnal trend reflects a significant daily variation; the HI increases after sunrise, peaks at midday (≈93°F) and decreases again after sunset. This mirrors what is known from natural solar heating and confirms the importance of temporal, as well as irradiance driven estimators in predictive modelling.

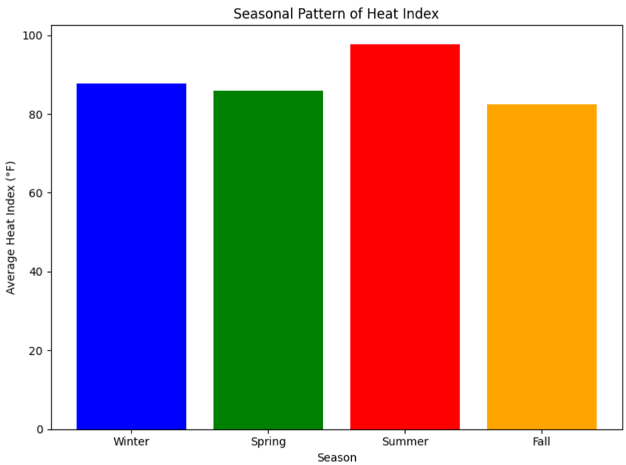

Fig. 5. Seasonal Pattern of Heat Index

Seasonal trend analysis indicated that HI peaked between May and June, averaging around 100°F, and decreased to around 80°F during December–January, validating the occurrence of a distinct pre monsoon heatwave period typical of northern India.

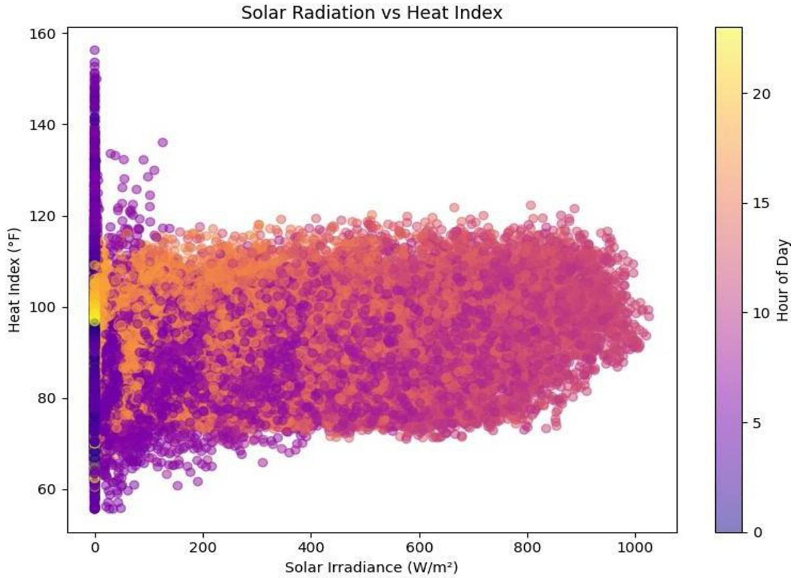

Fig. 6. Solar Radiation vs Heat Index

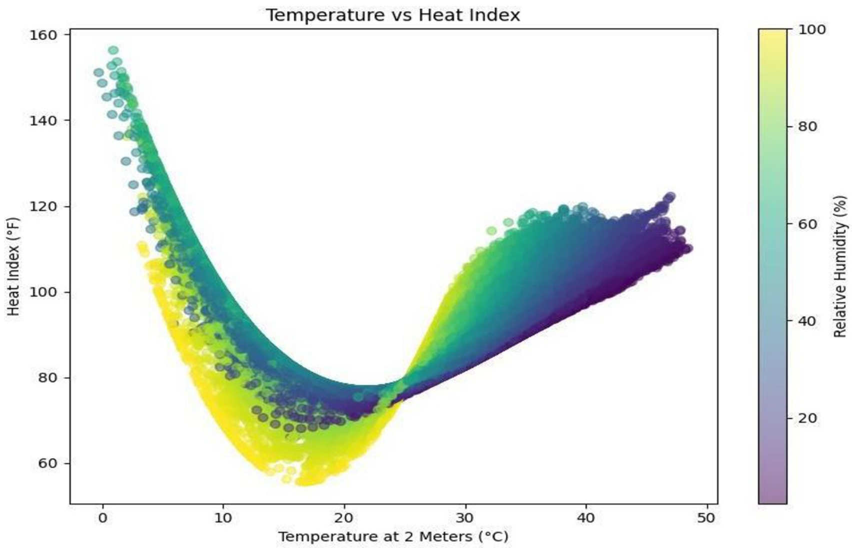

Fig. 7 Temperature vs Heat Index

Diurnal trends analysis showed a clear daily temperature cycle, with the lower HI values detected in the early morning hours and a steep rise which peaked between 13:00 and 15:00 hr., corresponding to daily maximum solar radiation. The Temperature–humidity relationship showed a strong nonlinear amplifying behavior, with higher humidity levels dramatically increasing perceived heat at constant temperature. All such analyses, herein, underscore the importance of radiative hygiene and temporal parameters on thermal stress variation contribution as well as provide substantial input for predictive AI based models that would seek to forecast artificial heat index.

Model Selection: The chosen machine learning and deep learning techniques applied were exploited for the salient advantages: different approaches to capture complex, nonlinear, and time dependent behaviors associated with environmental and thermal dynamics. Due to the multi-layer parameter dependence (e.g., temperature, humidity, wind speed and solar irradiance) a pure linear model is not enough. Ensemble methods, such as Random Forest, Gradient Boosting and CatBoost are successful for learning the nonlinear interactions and variable importance, while Support Vector Regression (SVR) achieves good generalization performance in high dimensional nonlinearly separable data. On the other hand, LSTM networks are well suited to learning temporal dependencies of time series data and so can model diurnal and seasonal variation in heat stress. These two when combined create a hybrid temporal model for forecasting heat index changes by taking advantage of both accuracy and interpretability of the obtained models.

Linear Regression (LR): Linear regression is a modelling technique that assumes a linear relationship between predictors and the response. It provides a reference basis to interpret rudimentary tendencies.

$$\mathbf{Y=\beta_0+\beta_1X_1+\beta_2X_2+...+\beta_nX_n+\epsilon}$$

where Y is the Heat Index, Xi are environmental variables, βi are coefficients, and ϵ is the error term.

Random Forest Regressor (RF): RF is an ensemble model which constructs a series of decision trees and averages the predictions in order to increase accuracy and decrease the risk of overfitting. It is capable of exploring nonlinear relationships and yielding important measures of features.

$$\hat{Y} = \mathbf{1/N}\sum_{i}^{N} T_{\mathbf{i}}\,\mathbf{(X)}$$

where T_i (X) is the prediction from the i^{th} tree and N is the total number of trees.

Gradient Boosting Regressor (GB): Gradient Boosting builds trees one at a time as well, with the next tree learning from and correcting errors made by the previous ones in an attempt to find the tree that corrects these collective errors using gradient descent. It is good at refining predictive performance

$$\mathbf{F_m(x)=F_{m\ 1}(x)+\gamma_m\ h_m(x)}$$

where $F_m(x)$ is the boosted model at iteration m, $h_m(x)$ is the weak learner, and γ_m is the learning rate.

Support Vector Regression (SVR): SVR will add complexity by using the kernel functions for mapping input data into high dimensions, then fit in a regression line within some margin of tolerance (ε insensitive zone.) It is better able to handle nonlinear and high dimensional relationships.

$$\mathbf{f(x)=w^T \phi(x)+b}$$

subject to $|y_i - f(x_i)| \leq \epsilon$ where $\phi(x)$ is the kernel transformation

Long Short-Term Memory (LSTM):

LSTM is an RNN with the ability to capture temporal dependencies and long-range dependencies in time series data. It employs gates to regulate the flow of information and the retention of memory.

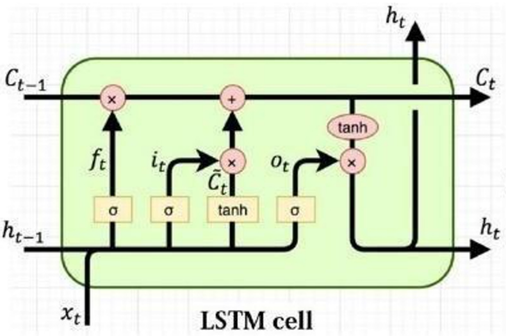

$$i_t = \sigma\left(x_t U^i + h_{t-1} W^i\right)$$
$$f_t = \sigma\left(x_t U^f + h_{t-1} W^f\right)$$
$$o_t = \sigma\left(x_t U^o + h_{t-1} W^o\right)$$
$$\tilde{C}_t = \tanh\left(x_t U^g + h_{t-1} W^g\right)$$
$$C_t = \sigma\left(f_t * C_{t-1} + i_t * \tilde{C}_t\right)$$
$$h_t = \tanh(C_t) * o_t$$

Fig. 8. LSTM Cell Architecture

Table 1. Different layers and its description

Sequence Length	Number of past time steps used for each prediction	48 (2 days of hourly data)
LSTM Layers	Two stacked LSTM layers	64 units (1st), 32 units (2nd)
Dropout Rate	Regularization to prevent overfitting	0.2 (after each LSTM layer)
Dense Layers	Fully connected layers following LSTM	32 neurons (ReLU) + 1 output neuron (Linear)
Loss Function	Objective minimized during training	Mean Squared Error (MSE)
Optimizer	Optimization algorithm used	Adam (learning rate = 0.0007)
Batch Size	Number of samples per training iteration	16
Epochs	Maximum number of training cycles	60
Callbacks	Early stopping and adaptive learning rate	EarlyStopping (patience=10), ReduceLROnPlateau (factor=0.5, patience=5, min_lr=1e 5)
Evaluation Metrics	Metrics used to assess performance	R^2, RMSE, MAE

5 Results

The model selection process indicated that tree based ensembles are superior to conventional regression and deep learning, in its prediction of the ACS like heat index. The highest prediction performance was obtained by Random Forest Regressor ($R^2 = 0.9993$, RMSE = 0.3231, MAE = 0.1409), showing an outstanding similarity between the prediction and the true response value of samples together with a great capacity of feature learning strength. Temperature at 2 meters was recognized as the most important variable, followed by All Sky Surface Longwave Downward Irradiance as the second more relevant one with respect to Heat Index. These findings validate both air temperature and radiative heat load as important contributors to the perception of heat stress

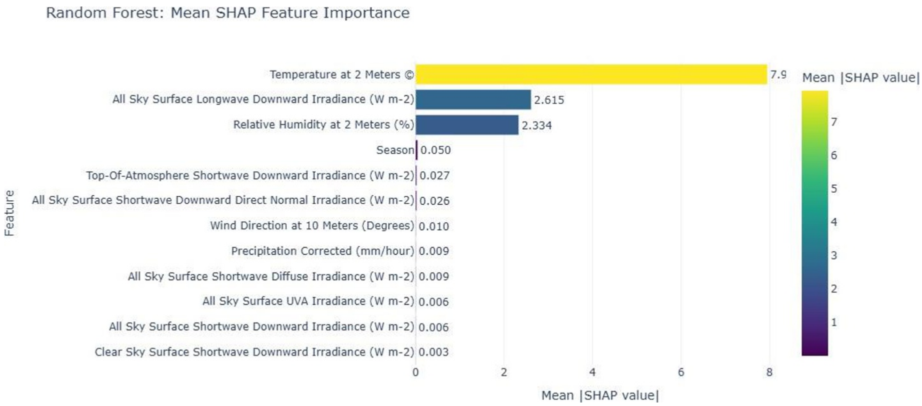

Fig. 9. Random Forest

Long Short Term (LSTM), R2 = 0.973, LSTM captured temporal time series dependency with a bit more error.

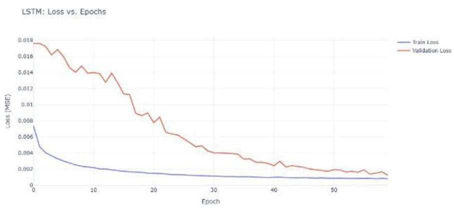

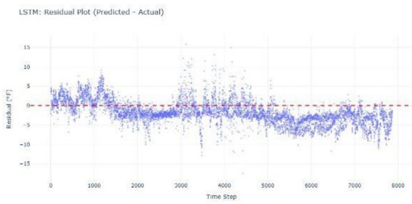

Fig. 10. LSTM: Loss vs. Epochs (Projected Actual)

Fig. 11. LSTM: Residual Pilot

From the SHAP plot, we would see that Temperature at 2 meters impacts the Heat Index prediction most and then All Sky Surface Longwave Downward Irradiance is next to Relative Humidity. Here the results indicate that temperature, radiation and humidity jointly determine the model predictions for heat stress.

The performance of LSTM is penalized by the few data available considering that only for one location 5 years of hourly environment observation were transmitted. This space time limitation was a barrier for the model to get a handle of large scale long term climate variations.

Model	**Accuracy (R^2)**	**Error (RMSE)**	**Error (MAE)**	**Remarks**
Random Forest (RF)	0.9993	0.3231	0.1409	Demonstrates exceptional predictive accuracy with minimal error; indicates strong nonlinear learning and robust feature utilization. Slight risk of overfitting due to near perfect R^2.
Gradient Boosting (GB)	0.9920	1.0699	0.7830	Performs very well overall; captures complex relationships but shows slightly higher error variance than RF, possibly due to residual bias in low variance conditions.
CatBoost	0.9983	0.4994	0.2642	Excellent accuracy with strong generalization. Handles categorical and continuous variables efficiently. marginally less precise than RF but more interpretable and stable.
Linear Regression (LR)	0.1535	10.9956	8.5444	Poor performance; unable to model nonlinear dependencies. High multicollinearity likely degraded coefficient stability and predictive power. Serves as a baseline model only.

Support Vector Regression (SVR)	0.9940	0.9227	0.3895	Strong performer with low bias and moderate variance. Effectively captures nonlinear patterns through kernel transformations, comparable to GB in stability.
LSTM Neural Network	0.973	1.797	1.247	Performs well but slightly lower than tree based models. Indicates good temporal learning but may require tuning (e.g., more epochs, deeper layers, or regularization) to reach full potential.

6 Future Implications

Although our proof of concept study has shown the potential of AI assisted environmental monitoring for the prediction of heat stress, it is constrained by receiving data from a single location and climatic region. Nevertheless, with extension of the dataset to other geographical areas and climate conditions, the completeness and transferability of models will be improved. Data across multiple locations (representing different microclimatic – **coastal, arid, temperate and high humidity zones)** would teach the algorithms a larger set of environmental thermal relationships. Such scale up of the intervention will not only increase prediction accuracy but also enhance generalizability to other health care and community settings elsewhere in India or analogous tropical countries.

Another interesting application of the models developed here is to provide the basis for a real time operational early warning system. In future work we intend to incorporate terrestrial sensors and processing within the system following real time meteorological data to adjust the prediction. From this live data, a predictive dashboard can be generated to predict 2 3 months of temperature and heat index changes. For example, it could automatically issue a recommendation to hospitals and public health departments with an early surge warning of higher temperature—even before the forecast calls for reaching critical thresholds—prompting preemptive actions **(e.g., increased cooling capacity; preloading of hydration protocols; curtailing energy loads)** to be considered. This real time decision support system would convert the model from a predictive research tool into a forecasting and preparedness instrument, that will allow healthcare institutions to anticipate and mitigate health impacts of upcoming heat stress events.

7 Conclusion

This study demonstrates an AI integrated environmental monitoring and decision support framework for managing extreme heat risk in healthcare and public use settings. Using a 5 year, high resolution (hourly) microclimate dataset from a hospital campus in Gurugram, India, the work combines exploratory heat risk profiling with predictive modelling to enable proactive operational responses during high risk periods. The results indicate that a substantial share of observed hours falls within elevated risk bands ("extreme caution" or "danger"), underscoring the need for campus level early warning and preparedness measures that can be triggered before conditions become hazardous. Across the evaluated models (Random Forest, Gradient Boosting, CatBoost, SVR, and LSTM), tree-based ensemble methods provided the strongest predictive performance for the Heat Index (HI), with Random Forest achieving the best fit (R^2 = 0.9993; RMSE = 0.3231; MAE = 0.1409). The LSTM model captured sequential dependencies in the time series (R^2 = 0.973; RMSE = 1.797), but with higher error under the present single site dataset and training configuration. Feature importance analysis indicates that near surface air temperature is the dominant predictor of HI, with radiative load (e.g., longwave downward irradiance) and relative humidity also contributing meaningfully consistent with the physical drivers of perceived heat stress in outdoor and semi outdoor microclimates. From an application perspective, the proposed framework links HI forecasts to implementable heat risk actions, including automated alerts, targeted HVAC operational adjustments, and site planning interventions (e.g., shaded movement corridors and vegetated surfaces) to reduce exposure along frequently used pathways. In this paper, HI is used as the primary modelling target because it supports public heat risk communication using commonly available meteorological inputs. WBGT is referenced as a complementary heat stress indicator in the literature and mitigation discussion (particularly for occupational guidance and for assessing interventions where radiant heat and airflow are critical), but it is not treated as the primary prediction target in the present modelling workflow.The study is limited by its reliance on a single campus location and climatic context, which constrains immediate generalizability. Future work should extend the framework to multi city and multi climatic datasets, adopt time consistent forecasting setups (with explicit lead times), and evaluate transferability across urban morphologies and exposure conditions. Additional improvements include integrating ground level sensor networks and operational data streams, validating predictions against observed health/service impacts where feasible, and expanding outputs from continuous HI prediction to risk classification and actionable threshold-based triggers suitable for real time institutional preparedness.

Conflict of Interest: The authors declare that they have no conflict of interest.

Funding Declaration: This research did not receive any specific grant from funding agencies in the public, commercial or not-for profit sectors.

Ethics Declaration: Not applicable.

Clinical Trials: Not applicable.

Data Availability Statement: Data will be available upon reasonable request.

References

1. National Weather Service (NOAA). "What is the Heat Index?"
2. India Meteorological Department. "FAQ on Heat Wave."
3. ISO. **ISO 7243:2017** Ergonomics of the thermal environment—Assessment of heat stress using the WBGT index.
4. NIOSH (Jacklitsch et al.). **Criteria for a Recommended Standard: Occupational Exposure to Heat and Hot Environments**, DHHS (NIOSH) 2016-106.
5. WHO Regional Office for Europe. **Heat-health action plans: guidance** (EuroHEAT), 2008.
6. Knowlton K. et al. "Development and Implementation of South Asia's First Heat-Health Action Plan in Ahmedabad (Gujarat, India)."
7. Hess J.J. et al. "Pilot Evaluation of the Impact of India's First Heat Action Plan on All-Cause Mortality."
8. Dasgupta R. et al. "Heat action plans in eight Indian cities: Knowledge gaps & opportunities for intersectoral heat governance." Indian J Med Res (2025).
9. NDMA (India). Heat-wave management / HAP preparedness & response material (includes note on guideline revisions and long-term measures).
10. ARTPARK @ IISc. "Heatwaves + Health Risk Prediction" (hyperlocal DL-based forecasting concept).
11. Ratnam J.V. et al. "Predicting maximum temperatures over India 10-days ahead using machine learning models." Scientific Reports (2023).
12. Suthar G. et al. "Prediction of maximum air temperature for defining heat wave… using machine learning approach." (2023).
13. Kacker K. et al. "Personalized heat stress early warning system…" Environment International (2025).
14. Vellingiri V. et al. Cool-roof/roof-intervention indoor temperature reductions in Ahmedabad (2020).
15. Hall et al. WBGT reductions under shade (~2–6°C reported range).